Experimental Investigation on Heating Performance of a Cold Climate Thermoelectric-Assisted Heat Pump

Yifeng HU[1*], Bo SHEN[1], Kyle R. GLUESENKAMP[1], Samuel F. YANA MOTTA[1], Sreenidhi KRISHNAMOORTHY[2], Don SHIREY[2]

1 Buildings and Transportation Science Division, Oak Ridge National Laboratory, Oak Ridge, TN37830, USA

2 Electric Power Research Institute, Palo Alto, CA 94304, USA

* Corresponding Author

ABSTRACT

To accelerate the electrification of air source heat pumps (ASHPs) in cold climates across the United States, various initiatives have been launched to enhance the effectiveness of ASHPs. One avenue of research involves incorporating thermoelectric (TE) technology into vapor compression refrigeration cycles. This study aims to assess the heating performance of a cold climate ASHP by employing TE modules as a liquid line subcooler. The tested system is a nominal 4.5-ton split heat pump utilizing R410A, equipped with a scroll compressor and an accumulator. An electronic expansion valve was employed for both cooling and heating modes. Two configurations of TE sub-coolers, one utilizing 2 TE bundles and the other 4 TE bundles, were integrated into the liquid line of the tested system. The heating performance of these configurations was evaluated. The results revealed that activating the TE subcooler led to a notable increase in total heat capacity, reaching 1318 W at -15.0 °C and 1164 W at -19.0 °C. The corresponding TE coefficients of performance (COPs) were 1.76 and 1.63, respectively. The activation of the TE sub-cooler resulted in a slight reduction in the overall system COP, with a decrease ranging from -2.6% to -4.2% for these two temperatures. The system COPs were measured at 2.10 and 1.86 for -15.0 °C and -19.0 °C, respectively. This prototype demonstrated a significant augmentation in heating capacity with a minimal sacrifice in COP.

1. INTRODUCTION

Based on the 2020 Residential Energy Consumption Survey (EIA, 2020), space heating stands out as the primary energy consumer in the U.S. residential sector, accounting for 42% of total energy usage. The predominant methods for space heating in residential areas are split air source heat pumps (ASHPs) or furnaces. In April 2023, the U.S. Department of Energy (DOE, 2023) announced a $250 million funding opportunity aimed at accelerating the domestic manufacturing of electric heat pumps.

However, conventional ASHPs encounter significant challenges when deployed in cold climate regions, including elevated discharge temperature and compression ratio, reduced efficiency and capacity, and issues related to frost formation and defrost power consumption penalties. In such regions, properly sizing a heat pump to meet the building's

cooling load often results in insufficient capacity to meet the heating load, necessitating the use of electric resistance auxiliary heating below -5˚C ambient temperature and leading to a notable decrease in seasonal heating efficiency. Conversely, sizing the heat pump to meet the peak heating load results in oversizing for cooling needs, causing noticeable on/off cycling losses during the cooling season and inefficient heating at moderate ambient temperatures.

Roth and colleagues (2009) proposed various strategies to enhance heat pump acceptance in cold regions, including incorporating multiple or modulating compressors, increasing outdoor coil capacity, implementing mechanical liquid subcooling, and optimizing both indoor and outdoor coil systems. An emerging research area involves integrating Thermoelectric (TE) technology into vapor compression refrigeration (VCR) cycles. TE heat pump (TEHP) systems, highlighted by Zhao and Tan (2014), offer advantages such as compact design, reliability, absence of mechanical parts, independence from a working fluid (e.g. refrigerants), and operation on direct current power. Despite TE modules' lower efficiency compared to traditional vapor-compression heat pumps, integrating TE cooling/heating at the system level is straightforward. Additionally, Qian et al. (2015) note TE cooling's highest system exergetic efficiency among various non-vapor compression technologies assessed.

Numerous studies (Vian and Astrain, 2009; Okuma et al., 2012; Schoenfield et al., 2012; Sarkar, 2013; Zhu and Yu, 2015; Jamali et al., 2017; Liu et al., 2019; Ghazizade-Ahsaee and Baniasad Askari, 2020; Wantha, 2020; Sánchez D, 2020; Aranguren, 2021; Casi Á, 2022) have integrated TE modules into VCR cycles to enhance system performance. Vian and Astrain (2009) developed a hybrid refrigerator combining TE and VCR technologies to stabilize temperature fluctuations in the super-conservation compartment and improve food preservation. Okuma et al. (2012) proposed a VCR system with integrated TE for efficient heating in cold climates, demonstrating improved efficiency and capacity. Wantha (2020) utilized a TE subcooler in an R134a refrigeration system, achieving a 24.3% improvement in overall COP by optimizing subcooling. Several studies focused on TE subcoolers in transcritical CO_2 cycles (Schoenfield et al., 2012; Sarkar, 2013; Jamali et al., 2017; Aranguren, 2021; Sánchez D, 2020; Casi Á, 2022). Zhu and Yu (2015) incorporated thermoelectric subcoolers and ejectors into an ASHP, while Liu et al. (2019) and Ghazizade-Ahsaee and Baniasad Askari (2020) applied them to transcritical CO_2 refrigeration cycles.

While TE heat pump technology has experienced notable growth in recent years, there is limited experimental data on its utilization for space heating. This study aims to address this gap by developing, demonstrating, and evaluating a novel configuration that cascades a split system ASHP with a solid-state TEHP. Experimental tests were conducted in dedicated psychrometric chambers under low ambient temperatures to showcase the enhanced heating performance of this prototype. The initiative is aimed at accelerating the electrification of ASHPs in cold climates within the United States.

2. EXPERIMENTAL SETUP

2.1 Description of the Tested Systems

Figure 1 depicts the schematic diagram of a residential ASHP incorporating a solid-state TEHP in heating mode. Experimental tests were conducted in psychrometric chambers to regulate indoor and outdoor air temperatures precisely. The tested system, a nominal 15.8 kW (4.5 tons) split heat pump using R410A, comprises indoor and outdoor sections typical in ducted whole-house residential applications. In the indoor section, an electronically commutated motor (ECM) blower draws air through an auxiliary coil (3 tons) and an indoor coil (4.5 tons) arranged in series. Temperature grids with nine thermocouples each measure air temperature at the inlet and outlet of the coils, along with humidity sensors. The outdoor section of the tested system includes a scroll compressor featuring three stages, outdoor coil, accumulator, and a reversing valve, with continuous operation at the highest stage during testing. Indoor coils are finned tube heat exchangers, while the outdoor coil adopts a micro-channel design.

The TE bundles, each containing 25 TE modules, were assembled (Figure 2). Power consumption of the blower and TEHP bundles is measured. Calibrated thermocouples along the refrigerant tube measure refrigerant temperatures at the inlets and outlets of the indoor and auxiliary coils. Refrigerant mass flow rate is quantified using a Coriolis flowmeter before an Electronic Expansion Valve (EEV) controlled by a Proportional-Integral (PI) controller to maintain a 6 °C subcooling at the TEHP's low-temperature side outlet. A suction line accumulator ensures saturated vapor enters the compressor. Pressure transducers and temperature sensors were installed at the compressor's inlet and

outlet. Power consumption of the compressor and outdoor fan was measured separately using power meters. Table 5 lists specified uncertainties for sensors and average uncertainties for cooling capacity and COP.

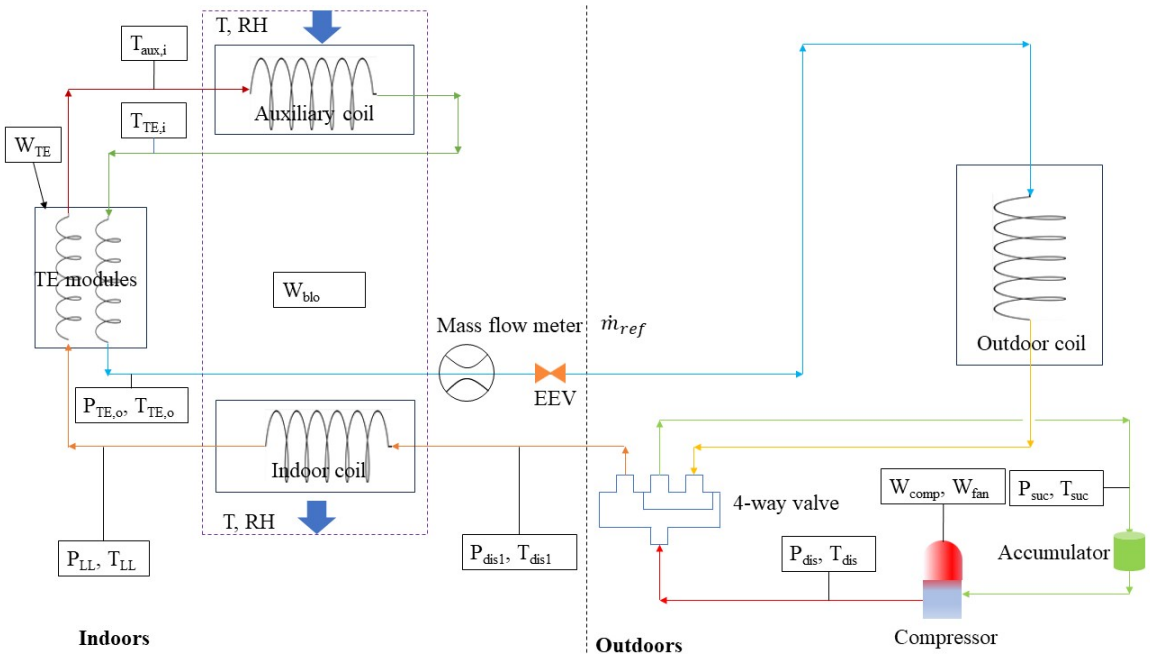

Figure 1: Schematic diagram of the tested system in heating mode (Hu et al. 2024)

Figure 2: One bundle of the TEHP setup

Table 1: Uncertainty analysis

Parameters	Range	Uncertainty
Thermocouple	-200-260 °C	±0.5 °C
Relative humidity	0-95%	±3%
Refrigerant pressure	0–69 bar	±0.25%
Refrigerant mass flow rate	0–500 kg/h	±0.2%
Compressor power	0-5 kW	±0.2% F.S.
TE, indoor blower, outdoor fan	0-1 kW	±0.2% F.S.
Heating capacity	0-16 kW	3.60%
COP	0-5.0	3.64%

Data on performance were documented for each condition, collected over a half-hour period once the unit achieved a steady state lasting more than thirty minutes. The experimental findings, averaged over this half-hour duration, are presented below. Figure 3 illustrates the prototype of the split system cascaded with a TEHP, equipped with two parallel TE bundles.

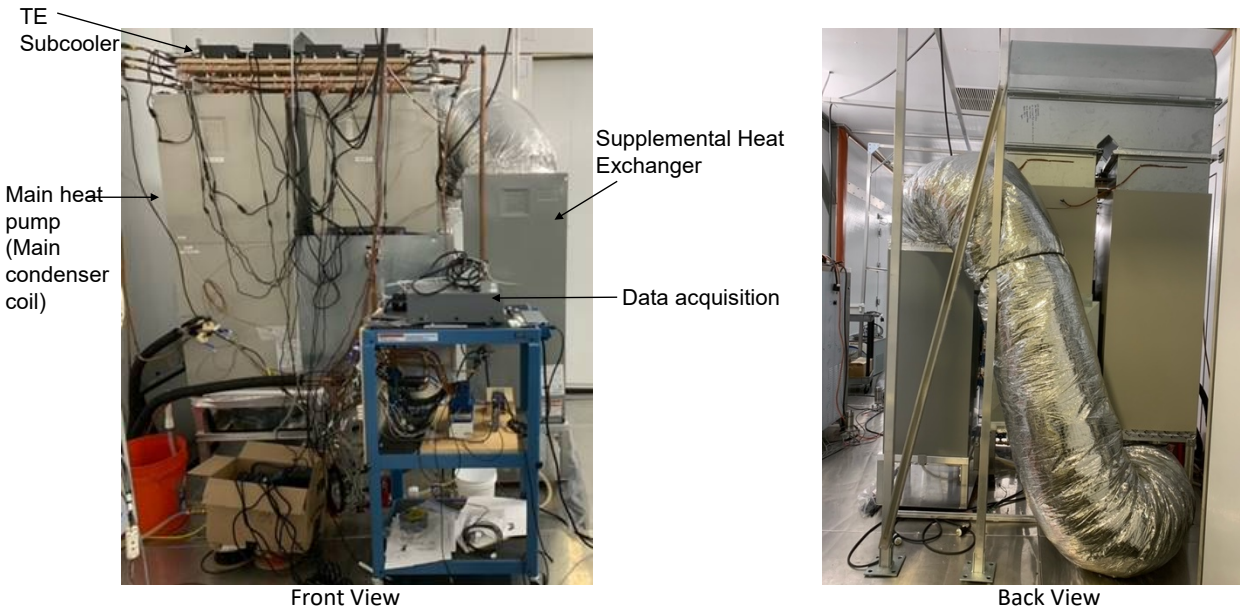

Figure 3: Prototype of a split system with a TEHP (two TE bundles)

2.2 Test Conditions and Matrix

Table 2 presents the testing parameters and matrix. The experiments were conducted with two distinct configurations of TEHP, adjusting the TEHP bundles (2, 4). Each set of tests (with TEHP On and Off) was conducted under identical indoor and outdoor conditions to enable straightforward comparison.

Table 2: Operating testing conditions and test matrix

Test	TEHP			Indoor air temperature, ◦C		Outdoor air temperature, ◦C	
	Bundle	Status	Power (W)	Dry-bulb	Wet-bulb	Dry-bulb	Relative humidity
1	2	Off	0	21.1	≤15.6	-15.0	70%
2		On	286				
3		Off	0			-18.0	
4		On	286				
5	4	Off	0			-15.0	
6		On	680				
7		Off	0			-19.0	
8		On	680				

Heating capacity can be calculated using two methods: utilizing air-side enthalpy or refrigerant-side enthalpy. With the TEHP integrated on the refrigerant side, the main approach for determining cooling capacity relied on refrigerant-side enthalpy, while the air-side method served as supplementary validation. During heating operation, the indoor coil operates as a dry-coil condition, and the temperature difference between the inlet and outlet of the indoor air handler acts as an indicator for comparing the relative change in heating capacity when the TEHP is active versus inactive. Total heating capacity can be calculated using the following equation:

$$\dot{Q}_{ref} = W_{TE} + \dot{m}_{ref}(h_{dis1} - h_{TE,o}) + W_{blo} \quad (1)$$

where W_{TE} indicates the power consumption of the TEHP, kW; $\dot{m}_{ref}$ denotes the refrigerant mass flow rate, kg/s; h_{dis1} signifies the specific enthalpy of the refrigerant at the inlet of the indoor coil, kJ/kg; $h_{TE,o}$ represents the specific enthalpy of the refrigerant at the outlet of the low side of the TEHP, kJ/kg. W_{blo} represents the power of the indoor blower.

The specific enthalpy of the refrigerant at the inlet of the indoor coil and the outlet of the low-temperature side of the TEHP can be determined using the refrigerant property function (NIST, 2022).

$$h_{dis1} = f(R410A, P_{dis1}, T_{dis1}) \quad (2)$$

$$h_{TE,o} = f(R410A, P_{TE,o}, T_{TE,o}) \quad (3)$$

where P_{dis1} and T_{dis1} represent the refrigerant pressure and temperature at the inlet of the indoor coil, and $P_{TE,o}$ and $T_{TE,o}$ represent the refrigerant pressure and temperature at the outlet of the low-temperature side of the TEHP, respectively. When the TEHP is operational, the TEHP capacity of the low-temperature side can be computed as follows:

$$\dot{Q}_{TE,l} = \dot{m}_{ref}(h_{TE,i} - h_{TE,o}) \quad (4)$$

where $h_{TE,i}$ represents the refrigerant specific enthalpy at the inlet of the low-temperature side of the TEHP, which can be determined using the following equation:

$$h_{TE,i} = f(P_{TE,o}, T_{TE,i}, R410A) \quad (5)$$

where $T_{TE,i}$ denotes the temperature at the inlet of the low-temperature side of the TEHP. The COP of the TEHP and the whole system can be calculated as the following equations:

$$COP_{TE} = \frac{\dot{Q}_{TE,l} + W_{TE}}{W_{TE}} \quad (6)$$

$$COP_{sys} = \frac{\dot{Q}_{ref}}{W_{blo} + W_{TE} + W_{comp} + W_{fan}} \quad (7)$$

where W_{fan} and W_{comp} represent the power consumption of outdoor fan and compressor, respectively.

3. RESULTS AND DISCUSSION

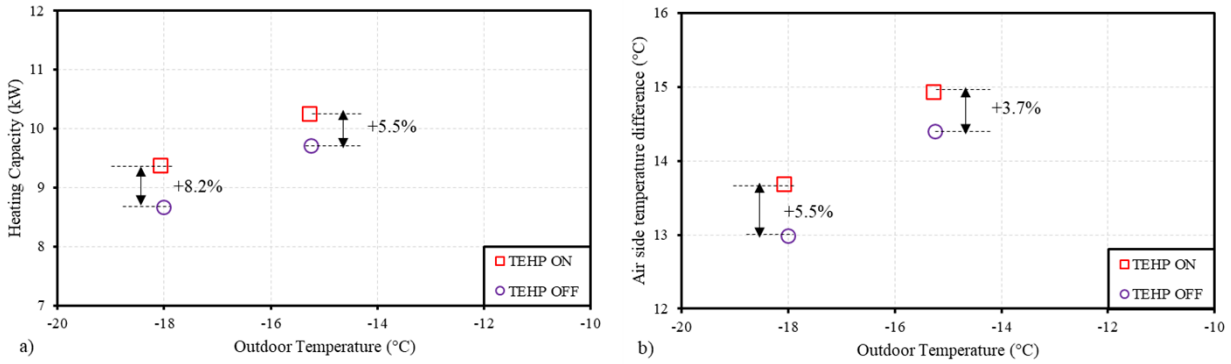

Figure 4: Comparison of the system heat capacity with 2 bundles of the TEHP

Figure 4 displays the heat capacity of the ASHP, depicting two sets of TEHP bundles in activated and deactivated states across two different ambient conditions. The activated TEHP exhibits an increase in heating capacity by 8.6% and 5.7% compared to the deactivated state, as indicated by the air side temperature difference, which is a crucial indicator of heating capacity. Nonetheless, the rate of increase from the air side is lower compared to that from the refrigerant side. Nevertheless, this increase exceeds the measurement uncertainty, suggesting a discernible upward trend.

In Figure 5, the COP for both the TEHP and the entire system is presented. With the TEHP power input fixed at 286 W, the TE sub-cooler generates a heating capacity of 509 W at -15.0 °C and 455 W at -18.0 °C, resulting in TEHP COP values of 1.78 and 1.59, respectively. Activation of the TE system leads to a total heat capacity increase of 532 W and 710 W at these two ambient conditions. It is noteworthy that TEHP activation introduces minor fluctuations in the system COP, ranging from -1.6% to 1.3% for these temperatures. Specifically, the system COP for the activated TEHP is 2.16 at -15.0 °C and 1.98 at -19.0 °C.

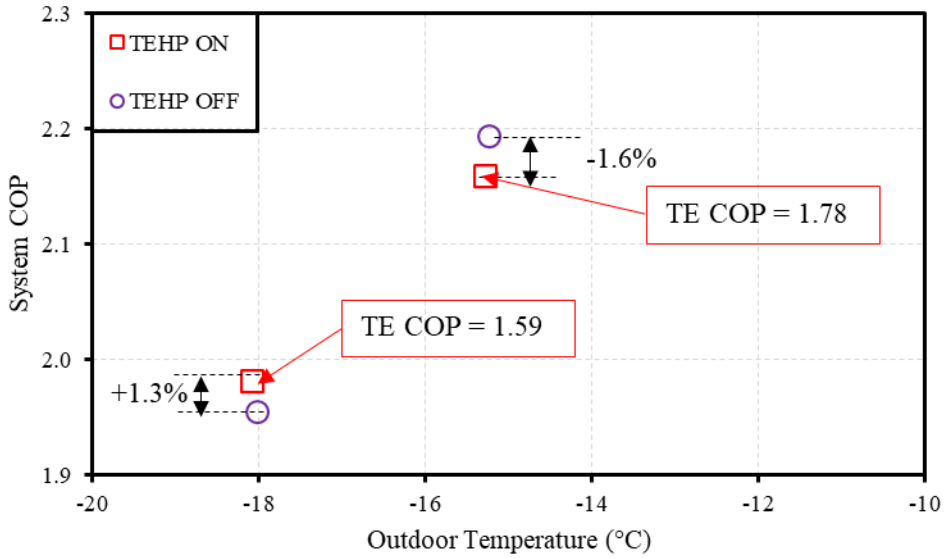

Figure 5: COP of the 2 bundles of the TEHP and system

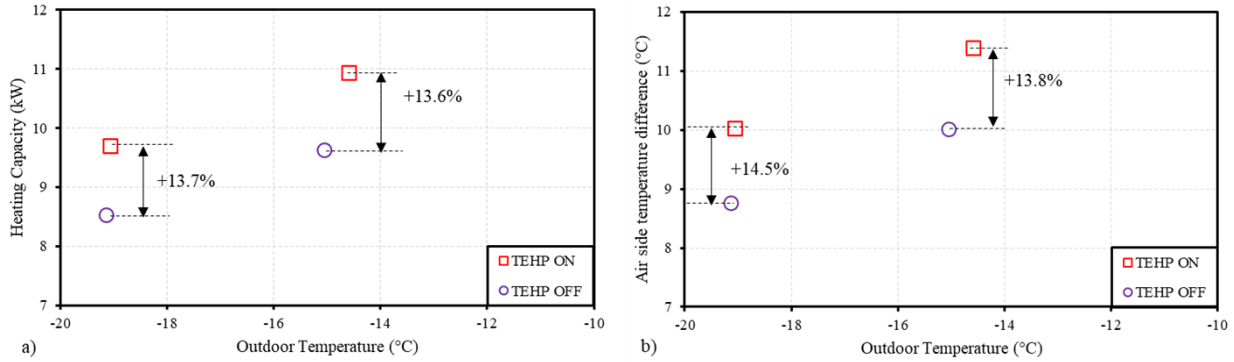

Figure 6: Comparison of the system heat capacity with 4 bundles of the TEHP

Figure 6 displays the ASHP's heat capacity, showcasing four TEHP bundles in both activated and deactivated states. Across both ambient conditions, activating the TEHP results in a roughly 13.6% increase in heating capacity compared to its deactivated state. The air side temperature difference, acting as an indicator of heating capacity, reinforces these capacity improvements, demonstrating a comparable upward trend.

In Figure 7, the COP of both the TEHP and the entire system is showcased. Maintaining a constant TEHP power input of 680 W, the TEHP generates a heating capacity of 1194 W at -15.0 °C and 1106 W at -19.0 °C, resulting in TEHP

COP values of 1.76 and 1.63, respectively. Activation of the TE system leads to a total heat capacity increase of 1318 W and 1164 W at these temperatures. However, activating the TEHP introduces a slight decrease in system COP, ranging from -5.0% to -3.1% for these two temperatures. Specifically, the system COP is 2.21 at -15.0 °C and 1.96 at -19.0 °C.

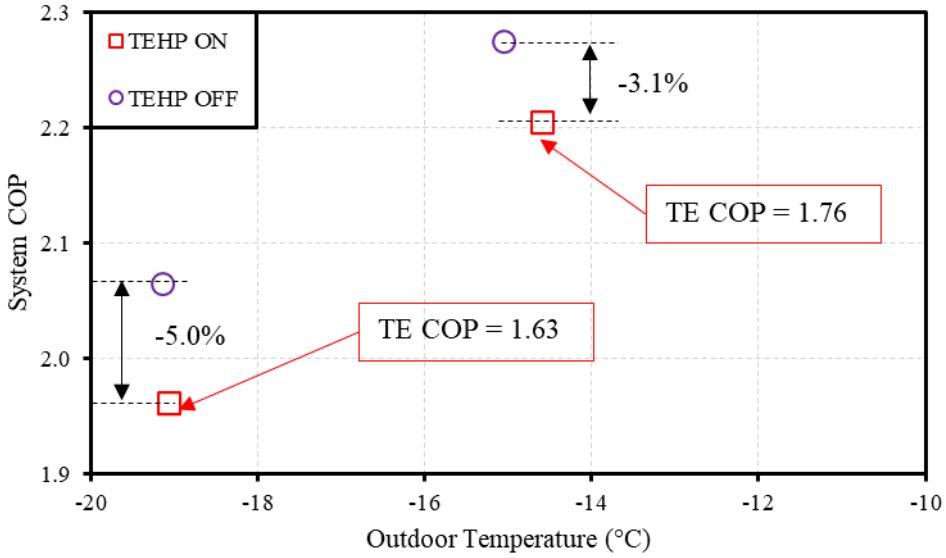

Figure 7: COP of the 4 bundles of the TEHP and system

4. CONCLUSIONS

An innovative prototype of a cold climate heat pump, integrating TEHP technology with a conventional split system ASHP, has been conceptualized, designed, and subjected to both experimental analyses. From the conducted studies, the following conclusions emerge:

- The COP of the TEHP remains relatively stable, fluctuating within the range of 1.59 to 1.76. This observation implies an increasing advantage of the TEHP over the ASHP as outdoor ambient temperatures decrease. This advantage stems from the declining efficiency of the ASHP in extremely low ambient temperature conditions.
- Incorporating the TEHP into the system leads to a continuous enhancement in the overall heating capacity. Activation of the TEHP demonstrates the potential to increase the heating capacity by up to 1.3 kW for the current system configuration, with only a marginal decrease in COP below an ambient temperature of -15 °C. This enhancement stands in contrast to the system's performance without TEHP activation.

NOMENCLATURE

Symbol		**Subscript**	
ASHP	air source heat pump	amb	ambient
COP	coefficient of performance	blo	indoor blower
ECM	electronically commutated motor	com	compressor
EEV	electronic expansion valve	dis	discharge
$\dot{m}$	mass flow rate	fan	outdoor fan
P	pressure	h	high-temperature side
$\dot{Q}$	heating capacity	i	inlet
RH	relative humidity	l	low-temperature side
T	temperature	LL	liquid line
TE	thermoelectric	o	outlet
TEHP	thermoelectric heat pump	ref	refrigerant
VCR	vapor compression refrigeration	sys	system
W	power	TE	thermoelectric

REFERENCES

Aranguren, P., Sánchez, D., Casi, A., Cabello, R., Astrain, D., 2021. Experimental assessment of a thermoelectric subcooler included in a transcritical CO_2 refrigeration plant. *App. Therm. Eng., 190:* 116826.

Casi, Á., Aranguren, P., Araiz, M., Sanchez, D., Cabello, R., Astrain, D., 2022. Performance assessment of an experimental CO2 transcritical refrigeration plant working with a thermoelectric subcooler in combination with an internal heat exchanger. *Energy Conver. Manag., 268:* 115963.

DOE, 2023. *Biden-Harris Administration Announces $250 Million to Accelerate Electric Heat Pump Manufacturing Across America.* U.S. Department of Energy, 1000 Independence Ave. SW, Washington, DC 20585.

EIA, 2020. *2020 RECS Survey Data.* U.S. Energy Information Administration, 1000 Independence Ave., SW, Washington, DC. 20585

Ghazizade-Ahsaee, H., Askari, I.B., 2020. The application of thermoelectric and ejector in a CO_2 direct-expansion ground source heat pump; energy and exergy analysis. *Energy Convers. Manage., 226:* 113526

Hu, Y., Shen, B., Wan, H., Gluesenkamp, K. R., Krishnamoorthy, S., Shirey, D. 2024. Heating Performance of a vapor compression heat pump cascaded with a thermoelectric heat pump. *App. Therm. Eng., 249:* 123397

Jamali, S., Yari, M., Mohammadkhani, F., 2017. Performance improvement of a transcritical CO_2 refrigeration cycle using two-stage thermoelectric modules in sub-cooler and gas cooler. *Int. J. Refrig., 74:* 105–15.

Liu X, Fu R, Wang Z, Lin L, Sun Z, Li X., 2019. Thermodynamic analysis of transcritical CO_2 refrigeration cycle integrated with thermoelectric subcooler and ejector. *Energy. Convers. Manage., 188:* 354–65.

NIST, *Refprop 10 - Refrigerants Properties Database*, 2022.

Okuma, T., Radermacher, R., Hwang, Y., 2012. A novel application of thermoelectric modules in an HVAC system under cold climate operation. *J. Electron. Mater. 41:* 1749-1758.

Qin, F., Xue, Q.F., Velez, G.M.A., Zhang, G.Y., Zou, H.M., Tian, C.Q., 2015. Experimental investigation on heating performance of heat pump for electric vehicles at -20 °C ambient temperature. *Energy Convers. Manage. 102:* 39–49.

Roth, K., Dieckmann, J., Brodrick, J., 2009. Heat pumps for cold climates. *ASHRAE J., 51* (2): 69-72.

Sánchez, D., Aranguren, P., Casi, A., Llopis, R., Cabello, R., Astrain, D., 2020. Experimental enhancement of a CO_2 transcritical refrigerating plant including thermoelectric subcooling. *Int. J. Refrig., 120:* 178–87.

Sarkar, J.,2013. Performance optimization of transcritical CO_2 refrigeration cycle with thermoelectric subcooler. *Int. J. Energy Res., 37:* 121-128.

Schoenfield, J, Hwang, Y., Radermacher, R., 2012. CO_2 transcritical vapor compression cycle with thermoelectric subcooler. *HVAC & R Res., 18:* 297–311.

Vian, J.G., Astrain, D., 2009. Development of a hybrid refrigerator combining thermoelectric and vapor compression technologies. *Appl. Therm. Eng., 29:* 3319-3327.

Wantha, C., 2020. Experimental investigation of the influence of thermoelectric subcooler on the performance of R134a refrigeration systems. *App. Therm. Eng., 180:* 115829.

Zhao, D., Tan, G., 2014. A review of thermoelectric cooling: materials, modeling and applications. *Appl. Therm. Eng. 66:* 15–24.

Zhu, L., Yu, J., 2015. Theoretical study of a thermoelectric-assisted vapor compression cycle for air-source heat pump applications. *Int. J. Refrig., 51:* 33–40.

ACKNOWLEDGEMENT

The US Department of Energy's Building Technologies Office provided the funding, while Charles Pierce and Tim Dyer assisted in establishing the experimental infrastructure.